Tutor/s

Dra. Laura Rodríguez Raurell
Departament de Química Inorgànica

Grau de Química

Treball Final de Grau

Au(I) supramolecular structures used in molecular recognition processes.

Estructures supramoleculars de Au(I) emprades en processos de reconeixement molecular.

Clara Baucells de la Peña

June 2015

Universitat de Barcelona

Campus d'Excel·lència Internacional B:KC Barcelona Knowledge Campus

*Muchos **fracasos** ocurren en personas que no se dieron cuenta lo **cerca del éxito que estuvieron***

Thomas Alva Edison

Aquesta és la primera vegada que "faig de química", fora de l'entorn més controlat que suposen les pràctiques. Per dir-ho així, durant aquest treball he fet coses que no sabia si sortirien bé, m'he hagut d'enfrontar amb problemes que en altres ocasions ja venien resolts. He après que de vegades aquesta incertesa a l'hora de saber què fer per a complir un objectiu pot ser estressant: diverses vegades m'he sentit frustrada per no poder assolit el que ens havíem proposat. La meva tutora, a part de guiar-me i acompanyar-me durant tot el treball, m'ha fet veure que no "és un fracàs", és un pas endavant. Per això, vull dedicar un agraïment especial per a la Dra. Laura Rodríguez. També vull destacar l'ajuda que m'han ofert, sempre de bona gana, la Dra. Raquel Gavara i la Elisabet Aguiló. Gràcies també a l'Albert Gallén per amenitzar les hores de laboratori amb les seves anècdotes, i per haver-me ensenyat i aconsellat en moments de dubte. Finalment, un agraïment molt especial al Pablo, per sempre donar-me força i ànims.

REPORT

CONTENTS

1. SUMMARY

In the latest years there has been an increasing interest in the study of certain organometallic gold (I) complexes, due to the great variety of supramolecular structures that they form. Through the establishment of intramolecular weak interactions a process of self-assembly occurs; structures such as fibres, micelles and vesicles have been reported and some have proven to be gelators. A wide range of applications have been envisioned for these complexes in several fields: medicine, materials chemistry, applications in detectors, light harvesting and catalysis.

In the work presented herein, the study of two families of organometallic gold (I) complexes is presented. The first family are neutral complexes with general formula [[Au(4-ethynylbipyridine)(L)], and the second are charged complexes with general formula [Au(N-methyl-4-ethynylpyridine)(L)]X, where X=iodide, triflate and perchlorate. The ligands L are phosphines DAPTA and PTA. The purpose of this work is to study several properties of these complexes to better understand their nature.

The aggregation process (or self-assembly) over time, as a function of concentration and the solvent will be studied for the first neutral complexes. In addition, molecular recognition studies with three lanthanide cations will be performed.

The synthesis and later characterization of complexes [Au(N-methyl-4-ethynylpyridine)(L)]X with X=iodide and triflate will be carried out. Several unsuccessful attempts to synthetize the complex with X=perchlorate will be described in detail. Finally, aggregation studies have been carried out: their solvatochromism has been studied and their supramolecular structures have been observed through optical microscopy.

Keywords: Gel, alkynyl ligand, Gold, aggregation, luminiscence, solvatochromism

2. RESUM

En els últims anys hi ha hagut una pujança en la investigació de certs complexos organometàl·lics d'or (I) degut a la varietat d'estructures supramoleculars que formen. Mitjançant un procés d'auto-assemblatge dirigit per l'establiment de forces intermoleculars febles, estructures tals com fibres, micel·les i vesícules han estat reportades, i alguns han demostrat tenir propietats gelificants. La gamma d'aplicacions visualitzades per aquests compostos abasta diversos camps, des de la medicina fins a la química de materials, passant per aplicacions en detectors, captació de llum o catàlisi.

En el Treball de Fi de Grau que aquí es presenta s'exposa l'estudi de dues famílies de compostos organometàl·lics d'or(I): la primera es tracta de complexos neutres de formula general [Au(4-ethynylbipyridine)(L)], i la segona són complexos carregat de fórmula general [Au(N-methyl-4-ethynylpyridine)(L)]X, on X=iodur, triflat i peclorat. Els lligands L són les fosfines DAPTA i PTA. L'objectiu del treball és l'estudi de diverses propietats d'aquests complexos per tal de comprendre millor la seva naturalesa.

Del primer compost s'estudiarà el procés d'agregació (o auto-assemblatge) a mesura que passa el temps, en funció de la concentració i del dissolvent. A més, es realitzaran estudis de reconeixement molecular enfront de tres cations lantànids.

Dels compostos de fórmula [Au(N-methyl-4-ethynylpyridine)(L)]X se'n realitzarà la síntesi per als contraions X=iodur i triflat i es caracteritzaran els productes amb diverses tècniques espectroscòpiques. Per al contraió X= perclorat es detallarà els diversos intents realitzats per a la seva síntesi, tot i que finalment no s'ha tingut èxit. Finalment, s'han realitzat estudis d'agregació mitjançant l'estudi del seu solvatocromisme i la observació de les estructures supramoleculars amb microscòpia òptica.

Paraules clau: Gel, lligand alquinil, or, agregació, luminiscència, solvatocromisme

3. INTRODUCTION

Gels are very present in our daily lives for their immense range of applications; products such as shampoo, toothpaste, hair gel and other cosmetics, as well as contact lenses are all gels derived from polymeric compounds. They have been known and used for centuries, though their applications extend far beyond: food, medicine, pharmacology, etc[1]. For example, agar was discovered in 1660, and was first used to make jelly, and two centuries after Robert Koch used it to culture bacteria. Due to this historical background and massive use, much research has been carried out on these gels, and the nature of these materials has been described in detail and widely reported.

On the other hand, gels derived from low molecular mass gelators (LMWGs), also called supramolecular gelators, despite being known for long time, have started to be actively investigated in the last three decades. This category includes both organic molecules and metalogellators. In general terms, a gel consists of a large amount of liquid (solvent, discontinuous phase) and a small amount of solid (gelator, continuous phase); the solvent molecules are immobilized within the gel matrix, formed by an elastic cross-linked network. In polymer gels the formation of the solid matrix is a result of physical or chemical cross-linking of the polymeric strands, made of covalent-bounded monomers. By contrast, in LMWGs the self-assembly occurs through a combination of non-covalent interactions such as π-π stacking, hydrogen bonding, hydrophobic-hydrophilic interactions and van der Waals' forces, forming thus entangled *Self-Assembled Fibrillar Networks* (SAFINs)[2]. The reason why supramolecular gelators have stirred attention is the wide variety of futuristic applications that have been envisioned for these materials. To date, uses in drug delivery for medical purposes [3-5], high technology[2,6-8], materials chemistry[9-11], use in light harvesting[12], sensing[13] or catalysis[1] has been reported. There is as well a classification according to the solvent immobilized: organogels and hydrogels. As indicated by the name, organogels consist on gelator molecules that immobilize organic solvents while hydrogels consist on gelator molecules that immobilize water.

Despite the development of organic-based gelators in the past two decades, it was only in the past decade that there has also been an increasing interest in the investigation of metal complexes as supramolecular metallogelators. The reason for the growth of interest stems from the availability and the diversity of metal–ligand coordination that could readily induce or control the self-assembly process of the gel formation and thereby influence the gel properties[14]. Also, the utilization of transition metal complexes as metallogelators has been found to exhibit interesting properties, such as optical[15], catalytic[16]. In particular, the use of discrete small-molecule complexes as metallogelators has been relatively scarce, and it was only recently that a number of reports on the gelation properties of metal complexes, mainly Au(I), Au (III) and Pt(II) derivatives, have appeared[6,17]. Rodriguez and co-workers reported[18] recently on luminescent hydrometallogels from gold (I) complexes where the metal ion is coordinated with PTA (1,3,5,Triaza-7-Phosphaadamante) or DAPTA (3,7- Diacetyl-1,3,7-traiza-5-phosphabicyclo [3.3.1.] nonane) and an alkyne group bounded to a pyridine. What makes these molecules exceptional is that they are the smallest molecules observed to have gelating properties. According to the authors, apart from the weak interactions mentioned before (π-π stacking, hydrogen bonding, hydrophobic-hydrophilic interactions, Van der Waals…) these molecules' aggregation tendency could be determined by the establishment of Au-Au interactions (aurophilic interaction) and interactions between alkynyl C≡C-py units. Aurophilic interactions are non-covalent interactions, and from amongst other metal-metal interactions, such as silver and copper, they are the strongest: they are estimated to be energetically similar to hydrogen bonds[19]. Both their luminescent properties have been studied as well as their aggregation behavior, and have demonstrated that small variations in the structure can induce different supramolecular assemblies in water, and even rods or vesicles can be obtained[20]. These metallosurfactants capable of forming vesicles are also of interest due to their amphiphilic nature. They display the properties characteristic to both, a surfactant (self-assembly and surface activity) and a metal ion (redox and catalytic property). Because of the supramolecular assemblies formed, they are promising candidates as nanosized reactors[21], amongst other applications.

These studies are the starting point of the work presented herein. In particular, studies of the resulting aggregation will be performed on the neutral complexes [Au(4-ethynylbipyridine)(L)] (L=PTA,DAPTA) (Figure 1), which have been provided by the research group. The presence of bipyridiyl units makes them potential candidates to be used in molecular

recognition processes of cations. For this, and due to the great and emerging interest on lanthanides and luminescent materials[22], the interaction of the gold complexes with Eu^{3+}, Yb^{3+}, Dy^{3+} will be studied.

In addition, the synthesis of [Au(N-methyl-4-ethynylpyridine)(L)]X (L=PTA,DAPTA; X=I^-, OTf^-, ClO_4^-) (Figure 2) will be carried out and their luminescent properties (absorbance and fluorescent emission) in different solvents and the resulting supramolecular assemblies will be studied; this way the impact of the counterion on the properties of the molecule's supramolecular package can be analysed.

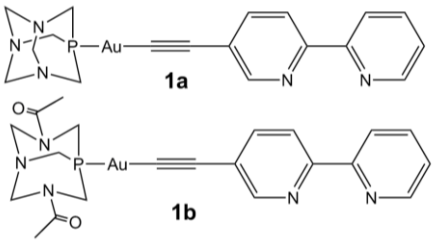

Figure 1. Molecules with general formula [Au(4-ethynylbipyridine)(L)] (L=PTA,DAPTA).

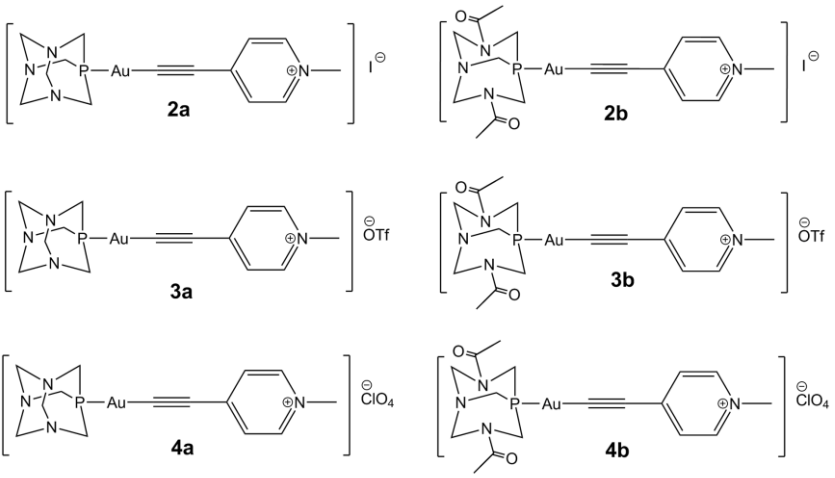

Figure 2. Molecules with general formula [Au(N-methyl-4-ethynylpyridine)(L)]X (L=PTA,DAPTA; X=I^-, OTf^-, ClO_4^-)

3.1. RECENT ANTECEDENTS

In previous reports [23,24], complexes **1a-b, 2a-b** and **3a-b** have been successfully synthetized and some of their properties have been studied. In general, they show some common properties. All of them form supramolecular structures that can be observed through diverse techniques such as Optical Microscopy and Scanning Electron Microscopy. In addition, they all show several absorption bands between 200-600 nm: a sharp band at 200-250 nm that is related to the aromatic system, and one or more bands between 300-600 nm that are related specifically to the monomeric or aggregate form (assignment is still not clear). Fluorescent properties are still to be studied. Moreover, all of them have proven to present molecular recognition with charged analytes.

Regarding complexes **1a-b**[23]: ^{1}H-NMR spectra were recorded for solutions of different concentrations. It was observed that as concentration rises the signals of the aromatic moiety disappear. Therefore, it was deduced that the variation of the intensity was caused by the intermolecular interactions established in the aggregation process, which provoke a variation in the relaxation time. Dynamic Light Scattering performed showed an average particle size of 50-100 nm for both **1a-b**. Using Scanning Electron Microscopy different type of structures like vesicles and dendrimers were observed. Molecular recognition studies performed with different transition metal cations showed a variation in the intensity of several bands between 300-400 nm in the absorption spectra.

Specifically for complexes **2a-b, 3a-b**[24]: the polarity effect on the absorbance has been studied, and a negative solvatochromism effect has been observed in bands which are suggested to be to halide-to-ligand and metal to ligand transitions. Dynamic Light Scattering measurements have been carried out on complex **2a**, showing an average particle size between 5 to 45 nm, depending on the concentration. Nevertheless, complex structures such as dendrimers, fibres and vesicles with sizes superior to 20 μm have been observed through optical microscopy. Using Scanning Electron Microscopy (SEM) images, which allow a better resolution, aggregates with squared and rectangular shapes were observed for complexes **3a-b**. In addition, molecular recognition studies with analytes ATP, Na_4ATP and sodium tripolyphosphate have been performed. It was observed that in the presence of the analytes, a red shift in the absorption spectra band was produced and absorption diminished at *ca.* 400 nm. That means that the aggregated forms are affected by the presence of guest molecules.

In the following sections the concepts of "molecular recognition" and "solvatochromism" will be briefly explained, as are closely related to these antecedents and the content of this work.

3.2. MOLECULAR RECOGNITION PROCESSES

The term molecular recognition refers to the specific interaction between two or more molecules through non-covalent bonding such as hydrogen bonding, metal coordination, hydrophobic forces, van der Waals forces, π-π interactions, electrostatic, etc. The fundamental basis for molecular recognition is provided by the potential energy surface that represents the interaction energy of two or more molecules in a cluster, as a function of their mutual separation and orientation. As the molecular size increases these interactions proliferate, making the system more complex and thus more difficult to study[25].

Molecular recognition is a fundamental step in different processes, e.g. in essential biological processes. Enzyme catalysis, cellular signalling, protein association, amongst others, involve the recognition between two or more molecules[26].

3.3. SOLVATOCHROMISM

Solvatochromism is defined as the ability of a chemical substance to change its colour by changing the solvent polarity. A shift to shorter wavelengths (blue shift, hypsochromic shift) when increasing the polarity of the solvent is called negative solvatochromism. The corresponding shift to longer wavelengths (red shift, bathochromic shift) is termed positive solvatochromism.

The solvatochromic effect refers to a strong dependence of absorption and emission spectra with the solvent polarity. Since polarities of the ground and excited state of a chromophore are different, a change in the solvent polarity will lead to different stabilization of the ground and excited states, and thus, a change in the energy gap between these electronic states (Figure 3). Consequently, variations in the position, intensity, and shape of the absorption spectra can be direct measures of the specific interactions between the solute and solvent molecules[27].

Charge-transfer transitions have found to be highly dependent on the polarity of the solvent. If the ligand molecular orbitals are full, charge transfer may occur from the ligand molecular orbitals to the empty or partially filled metal d-orbitals (LMCT). If the metal is in a low oxidation state (electron rich) and the ligand possesses low-lying empty orbitals then a metal-to-ligand charge transfer (MLCT) transition may occur. The absorptions that arise from these processes are called charge-transfer bands[27].

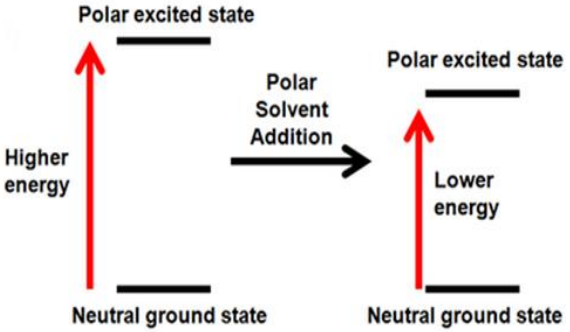

Figure 3. Solvatochromism effect: stabilization of the excited state due to the polarity of the solvent.
(Melissa A. Rivera , 3/5/15 via ChemWiki, Creative commons attribution)

4. OBJECTIVES

The aim of this work is the synthesis and characterization of several cationic alkynyl gold (I) complexes containing a water soluble phosphine and pyridine groups. Firstly these compounds will be synthetized according to methods proposed in the bibliography and characterized by different techniques. Solvatochromism studies will be performed, and the aggregated structures formed in the different solvents will be studied through optic microscopy.

In addition, molecular recognition studies of lanthanides will be performed by using another set of neutral gold (I) complexes provided by the research group. Also, the formation of aggregates will be analysed over time, concentration and in different solvents. The aggregated samples will be used as hosts in molecular recognition studies with different lanthanide cations.

5. STUDIES ON COMPLEXES WITH GENERAL FORMULA [AU(4-ETHYNYLBIPYRIDINE)(L)] (L=PTA,DAPTA)

Compounds **1a** and **1b** are neutral hydrosoluble complexes. In previous works done with those molecules it was proven that aggregation occurs through the formation of either small vesicles or long dendritic chains[23]. It was also demonstrated that their absorbance in solution is affected by the presence of cations such as Cu^{2+}, Co^{2+}, Fe^{3+} and Ni^{2+}, and it is suggested that they possibly coordinate to the bipyridine system with a 1 (cation):3 (gold complex) stoichiometry.

In this section the influence of some factors over the aggregation of compounds **1a** and **1b** will be analysed in more detail, and molecular recognition studies with lanthanide cations will be carried out. Compounds **1a** and **1b** were not synthetized, as they were provided by the research group.

5.1. AGGREGATION PROCESS OVER TIME

Previous research carried out on similar molecules show that when the aggregation process takes place, a variation on the absorption spectra occurs[17,23,24]. To corroborate this fact, solutions of different concentration of complexes **1a** and **1b** were prepared and the absorption and fluorescence emission spectra were recorded over time.

As it can be seen in figure 4, both compounds show maximum absorbance peaks at 310 nm and 360 nm, which decrease in intensity when aging. This tendency is observed in all concentrations. Studies[17] show the band at 240 nm is also present in the free phosphine ligand and has been tentatively assigned to phosphine centered intraligand transitions, while the intense absorption at *ca.* 265-285 nm is assigned to intraligand (IL) π-π* (C≡C-bipy) transitions. Comparison with litherature[28] let us also suggest that the band at 310 nm could be associated to metal-perturbed π-π* (C≡C-bipy) transitions, related to the monomeric form, while the band at 360 nm involves aurophilic interactions (possibly being σ*(Au-Au) → π* transitions[18]), therefore related to the aggregate.

According to this, it would be expected that the band at 310 nm decreases while the band at 360 nm increases when the aggregation is favoured. The recorded absorption spectra of a $2.5 \cdot 10^{-5}$ M solution of **1a** at different times show a fast disappearance of the band a 310 nm, while the variation of the aggregate's band is not so important. On the contrary, the recorded variations recorded for **1b** are slightly different, since the observed changes on the monomeric absorption band are not so fast (Figure 4).

The decrease of the monomeric band suggests that aggregation occurs over time. What does not seem to agree is the decrease of the band at *ca.* 360 nm. A possible hypothesis to explain this fact is that, as it is formed, the aggregates precipitate in the medium and so their absorption is not recorded. This hypothesis is supported by the fact that small yellow precipitates could be observed by naked eye.

Fluorescent emission spectra have been recorded at λ_{exc}=310 nm and λ_{exc}=360 nm. Excitation at λ_{ex}=310 nm show an emission spectra with a broad band at *ca.* 420 nm, which decreases in intensity over time. When exciting at λ_{ex}=360 nm the emission spectra show a band at *ca.* 430 nm and another band at *ca.* 630 nm for both compounds. When aging, all bands diminish in intensity (Figure 5). This behavior is in good agreement with the results of the absorbance spectra.

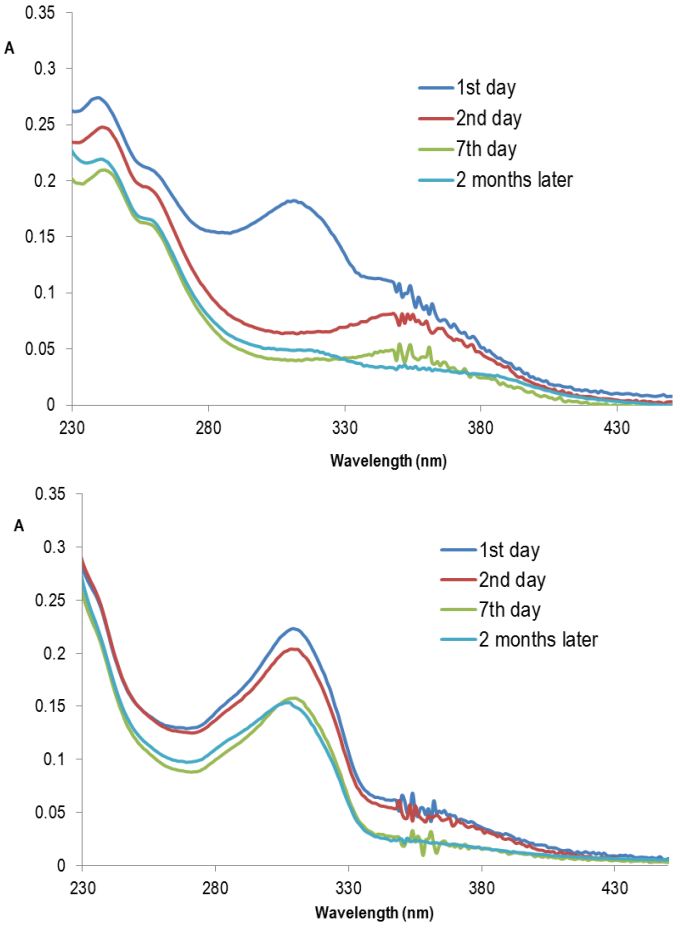

Figure 4. Absorption spectra over time for compounds **1a** (top) and **1b** (bottom)

Excitation spectra recorded show that emission at *ca.* 430 nm corresponds to the monomer (λ_{max}=320 nm) while emission at *ca.* 600 nm corresponds to the aggregate (λ_{max}=360 nm). This emission red shift of the aggregate has been described in previous works[17]. Thus, exciting at c.a. 310 nm only the emission of the monomer can be observed, but when exciting at c.a. 360 nm both the emission of the monomer and the aggregate can be observed, as both absorb at this wavelength.

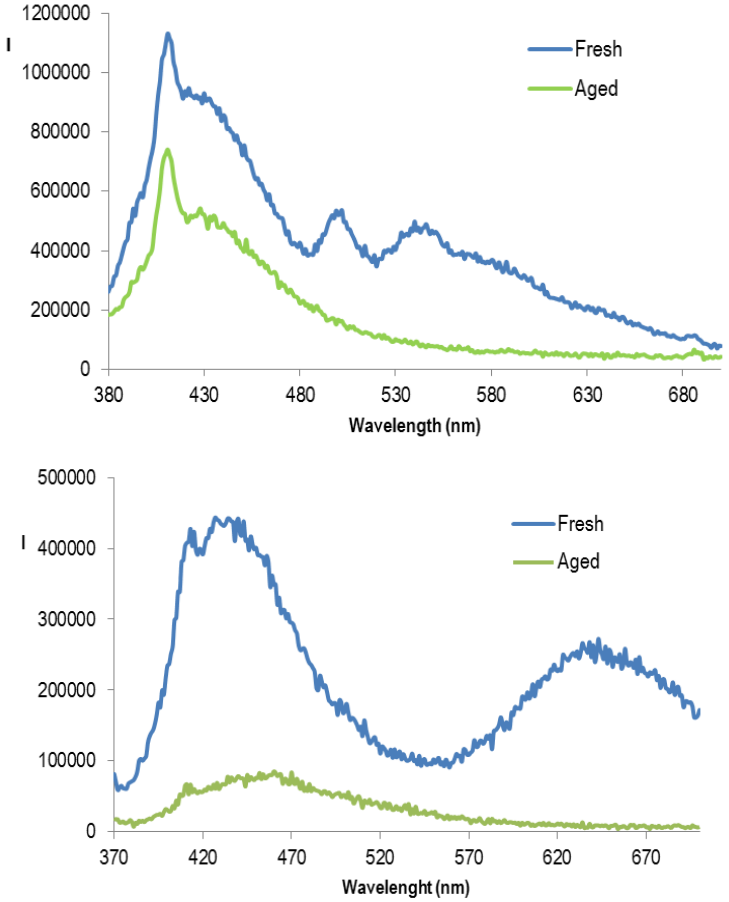

Figure 5 .Emission spectra with λ_{ex}=360 for compounds **1a** (top) and **1b** (bottom)

5.2. AGGREGATION PROCESS AS A FUNCTION OF CONCENTRATION

The aggregation of these molecules has been also studied at different concentrations ($2.5 \cdot 10^{-5}$, 10^{-4} and $5 \cdot 10^{-4}$ M). The fluorescent emission of $2.5 \cdot 10^{-5}$ M solution was not significant. On the other hand, for $5 \cdot 10^{-4}$ solution the absorbance was too high and the baseline was not good due to the presence of aggregates, which scatter the light. When exciting at ca. 360 nm, both 10^{-4} M and $5 \cdot 10^{-4}$ M solutions show bands at ca. 430 nm (monomer) and ca. 630 nm (aggregate), which change with the concentration. As depicted in figure 6, the aggregate predominates at higher concentrations, while the monomer is more abundant at lower concentrations.

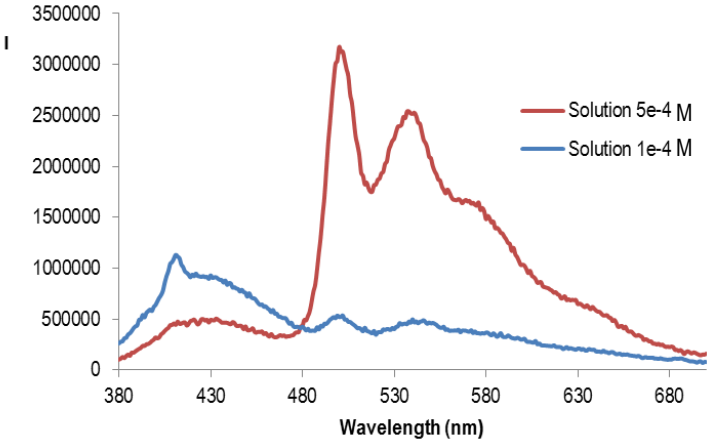

Figure 6. Emission spectra with λ_{ex}=360 nm for compound **1a** at concentrations $5 \cdot 10^{-4}$ M(red) and 10^{-4} M (blue)

This behaviour is in agreement with the expected: at more concentrated solutions the monomers are more likely to establish interactions between them, forming thus the aggregates.

5.3. AGGREGATION PROCESS AS A FUNCTION OF THE SOLVENT

It has been observed that certain solvents play an important role in the process of aggregation of similar complexes[29]. If compound **1** is dissected, we find that it has some amphiphilic character: phosphines are hydrosoluble, while the bipyridine system will be better solved by organic solvents. To study the effect of the solvent on the aggregation, complexes **1a** and **1b** were dissolved in a mixture of different percentages of D_2O and DMSO-d_6 and ^{1}H-NMR and ^{31}P-NMR were recorded. ^{1}H-RMNs of complex **1b** are shown in figure 7:

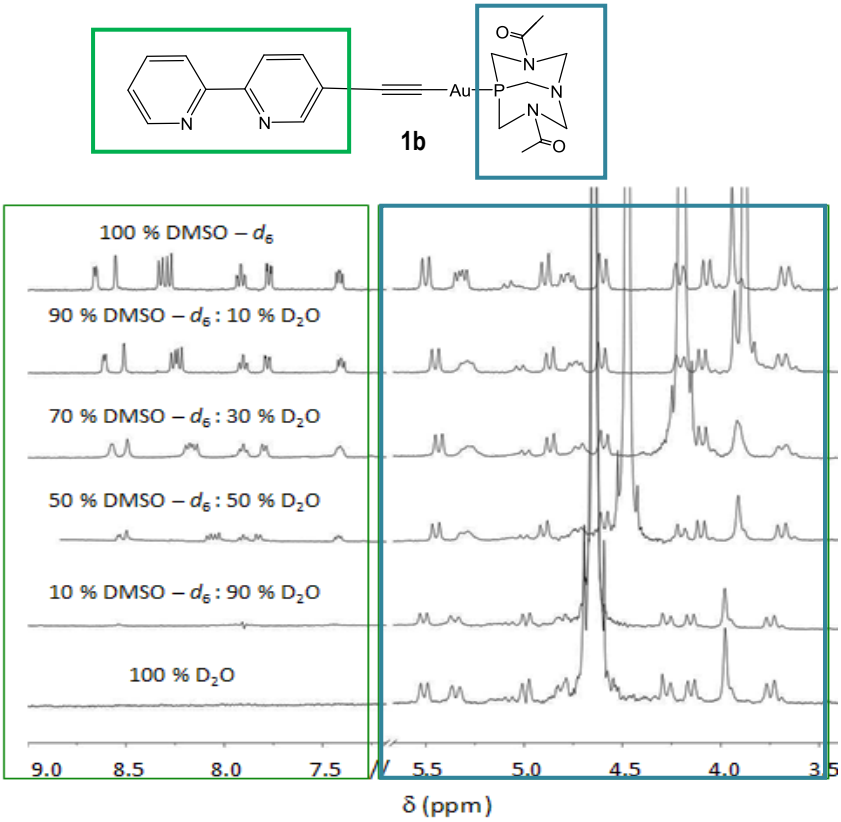

Figure 7. ^{1}H-NMR spectra of compound **1b** in different % of D_2O /DMSO-d_6

As it can be seen, signals between 9.0 ppm and 7.5 ppm, which correspond to the protons of the bipyridine system disappear progressively when increasing the percentage of D_2O. Signals disappear when their corresponding protons do not have rotational freedom, so that indicates that water induces aggregation in a form where bipyridines have a restricted position. That is in good agreement with the predicted behaviour: given that bipyridines are hydrophobic, they pack closely to each other through hydrophobic-hydrophobic interactions (pointing towards the inside of the aggregate), while phosphines are in contact with water. ^{31}P-NMR spectra (see appendix) support these conclusions and the observation of two different environments, that may correspond to the more and less (or monomeric) aggregated samples.

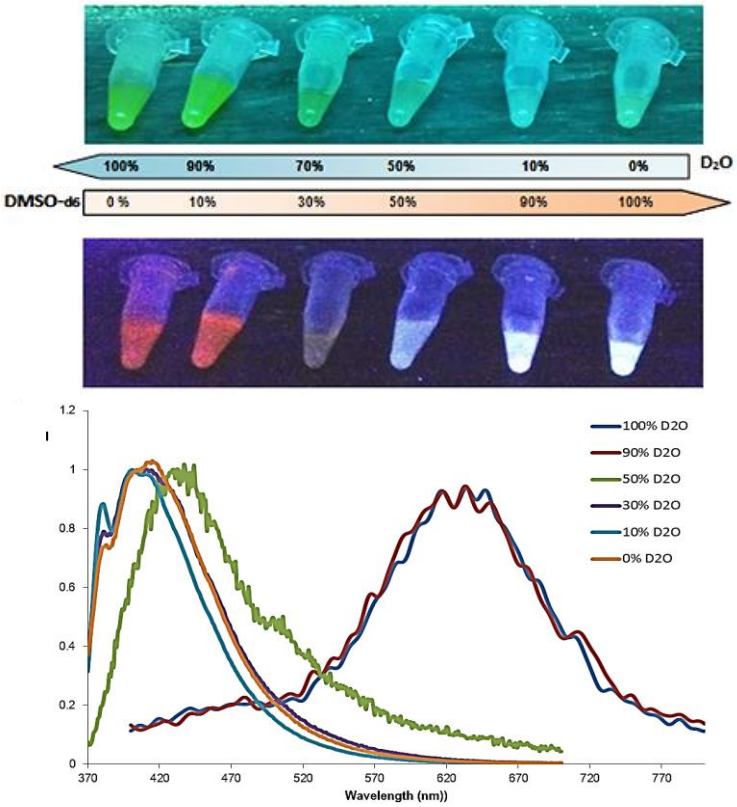

Figure 8. Red shift in emission when rising % of D_2O for complex **1b**. In the upper part, images of the variation of colour under visible and UV light . At the bottom, normalized graphic of fluorescence emission.

Emission spectra of the different solutions were recorded and it can be seen that emission at *ca.* 360 nm show an interesting tendency, which is in agreement with the observed in ^{1}H-NMR spectra: the emission band at 430 nm completely disappears when the percentage of D_2O rises to 90%, and a new band at *ca.* 630 nm appears (Figure 8). As explained in section 5.1, the bands at *ca.* 430 nm and *ca.* 630 nm correspond respectively to the monomeric and the aggregate emission. Thus, the spectroscopic information confirms the NMR results: aggregation is induced in water. Both compounds **1a** and **1b** show this tendency. The variation on the emission colour can be seen at naked eye when exposing the solutions to UV light (Figure 8).

5.4. MOLECULAR RECOGNITION

Molecular recognition studies were performed with complexes **1a**-**b** and different lanthanide cations: Eu^{3+}, Dy^{3+} and Yb^{3+} nitrate salts. To that end, $5\cdot10^{-4}$ M solutions of **1a** and **1b** in water were prepared and increasing amounts of 0.05 M solutions of the corresponding lanthanide nitrate were added. The emission spectra (λ_{exc}=360 nm) was recorded after every addition. The objective of this study is to collect information about the intermolecular interactions established between compounds **1a-b** and other molecules, and to test if it is possible to form new heterometallic supramolecular materials that could present high quantum yield and red emission. Lanthanide cations have been chosen because of their wide applicability in several fields: optical amplification and signal transmission for telecommunication, fluorescent dyes, light-emitting diodes, and in biological assays[22].

In general, in all the titrations carried out, the emission rises at *ca* .430 nm with larger equivalents of Ln^{3+} added in the solution (Figure 9). As seen in section 5.1, this band corresponds to the monomeric form, so this increase indicates that the monomeric species is being formed. Variations observed in the aggregate band, at *ca.* 600 nm, are less important mainly due to the higher emissive properties of the monomer with respect to the aggregate. The driving force of these variations is the existence of an interaction between the gold complexes and the cations, probably giving rise to heterometallic structures.

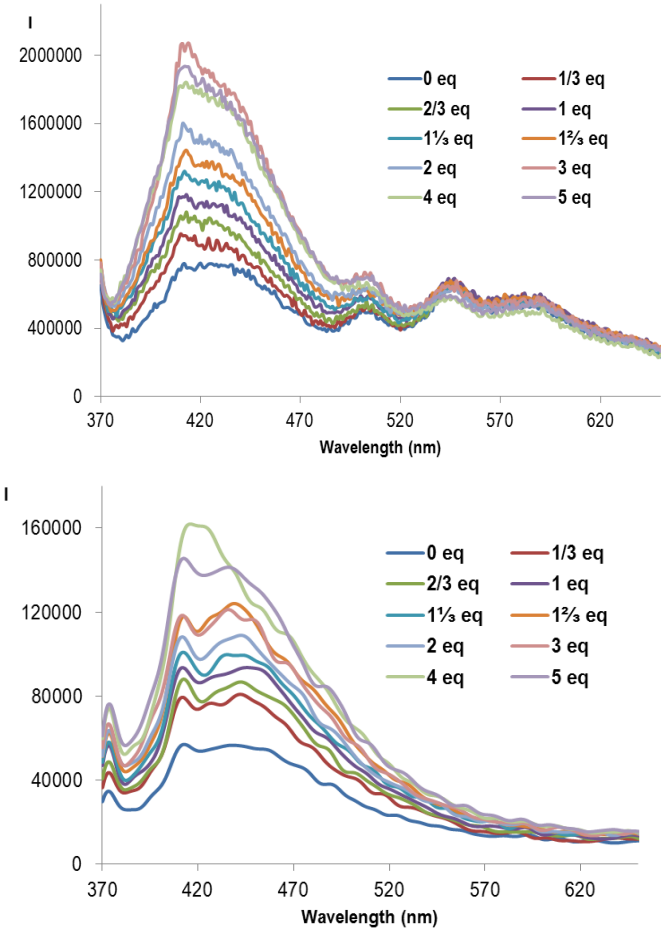

Figure 9. Emission spectra between 375 nm and 700 nm of compounds **1a** (top) and **1b** (bottom) as Yb^{3+} is added.

As mentioned in the introduction, the process of aggregation of these molecules involves the establishment of non-covalent interactions such as Au···Au, Van der Waals, π···π stacking, etc. As these interactions are weak, they can be easily modulated in the presence of other molecules. A hypothesis is that the nitrogens of the bipyridine system coordinate with the lanthanides, which results in the disaggregation of compounds **1a** and **1b,** thus raising the emission of the monomer while lowering the aggregate's band. Another remarkable fact is that the variation of emission intensity is proportionally the same for **1a** and **1b**, so the type of

phosphine does not affect to the molecular recognition process. More detailed studies are required in order to determinate the most important intermolecular interactions involved in the process and the coordination of the complex formed with the lanthanides.

6. STUDIES ON COMPLEXES WITH GENERAL FORMULA [AU(N-METHYL-4-ETHYNYLPYRIDINE)(L)] X (L=PTA,DAPTA), (X=I⁻, OTF⁻, CLO$_4^-$)

Compounds with general formula [Au(N-methyl-4-ethynylpyridine)(l)] X (L=PTA, DAPTA), (X=I-, OTf-) are hydrosoluble complexes that form supramolecular assemblies . Previous works[24] carried out with them revealed that their properties are highly sensitive to little variations in the molecule structure and that they interact with negatively charged analytes, possibly through electrostatic and π- π interactions. In this section the synthesis of complexes **2a**, **2b**, **3a** and **3b** through a validated synthetic route will be explained, as well as an attempt to synthetize compounds **4a** and **4b**. In addition, the influence of the solvent polarity on their properties will be studied, and the supramolecular structures they form will be observed through Optic Microscopy.

6.1. SYNTHETIC ROUTE

The synthetic route followed to obtain complexes **2a, 2b, 3a, 3b, 4a** and **4b** will be explained, as well as their characterization. Compounds **2a-b** and **3a-b** were successfully obtained, but it was not possible to obtain compounds **4a**-**b**.

All the manipulations were done under N_2 atmosphere using Schlenk techniques, and were kept protected from the light with aluminium foil.

6.1.1. SYNTHESIS OF [AU(N-METHYL-4-ETHYNYLPYRIDINE)(L)]I

The synthesis of the compounds **2a-b** requires several steps. The first one is the synthesis of the corresponding organic ligand (Scheme 1) and the following coordination with the organometallic gold (I) derivative, which contains the phosphine L (L=PTA, DAPTA) (Scheme 2).

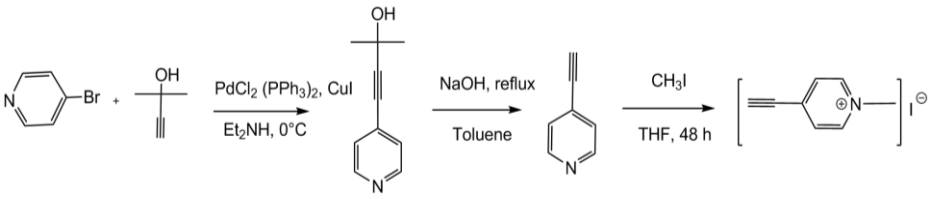

Scheme 1. Synthesis of N-methyl-4-ethynylpyridinum iodide

The procedure described in literature [30, 31] was followed to obtain 4-ethynylpyridine in an overall yield of 72%. The first step consists on a Sonogashira reaction, which is a coupling reaction where Pd acts as a catalyst and Cu(I) as a cocatalyst. $NHEt_2$ is necessary to deprotonate the alkynyl group. The following is the dehydrogenation of the alcohol, resulting into the ketone and a terminal alkynyl. The final reaction consists on the methylation of the 4-ethynylpyridine, which turned out to be highly time-dependant: after 6 hours the yield was only *ca.* 1%, after 24 hours the yield was 14%, and after 2 days it surprisingly increased to 53%. The final compound obtained was so pure that long crystals were directly formed in the reaction mixture. ^{1}H-NMR and IR were carried out to characterize the product. ^{1}H-NMR showed four characteristic signals at 9.18, 7.98, 4.60 and 3.93 ppm, corresponding to protons $H_{pyr-\alpha}$, $H_{pyr-\beta}$, N-CH_3 and C≡C-H respectively. IR showed a band at 2104 cm^{-1}, corresponding to the C≡C vibration.

The method described in literature was followed to obtain the gold (I) phosphine precursor [Au(acac)(L)], L=PTA,DAPTA [32, 33,34] . The general procedure is shown in scheme 2.

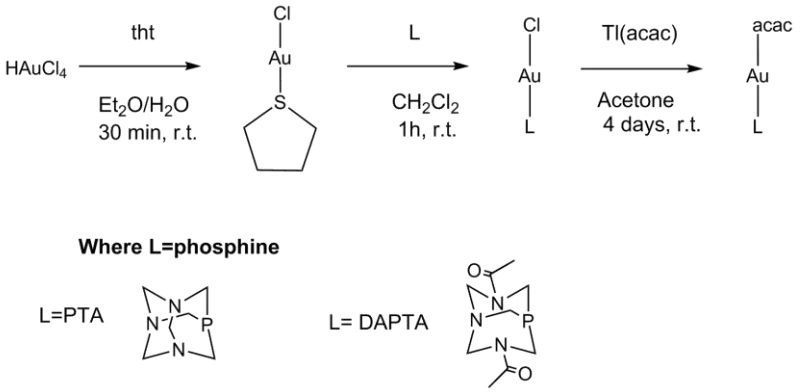

Scheme 2. Synthesis of [Au(acac) (L)] with L= phosphines PTA and DAPTA

In the first reaction, trivalent gold is reduced to monovalent gold while ethanol is oxidized to ethanal, and tetrahydrofuran (tht) is introduced as a ligand. Secondly tht is substituted by the phosphines PTA or DAPTA, as these phosphines are great coordinating agents to gold atom. Finally, ligand Cl^- is substituted by the acac group, as a good terminal alkynyl extractor. This last step of the sequence had a yield of only 31%, diminishing so the overall yield of the reaction to 12%. Future studies should be performed to improve the obtaining of [Au(L)(acac)]. IR was done to check the proper synthesis and verified the presence of carbonyl groups of the acac ligand.

To finally synthetize [Au(N-methyl-4-ethynylpyridine)(L)]I , N-methyl-4-ethynylpyridine and [Au(acac)(L)] are used as reagents (Scheme 3). This route is known as the "acac method"[35]: from a synthetic point of view, the reaction of an acac complex with a protic acid AH enables the coordination of its conjugate base A in the coordination position(s) previously occupied by the acac ligand. In this case, N-methyl- 4-ethynylpyridinum iodide acts as the acid, losing its terminal alkynyl proton.

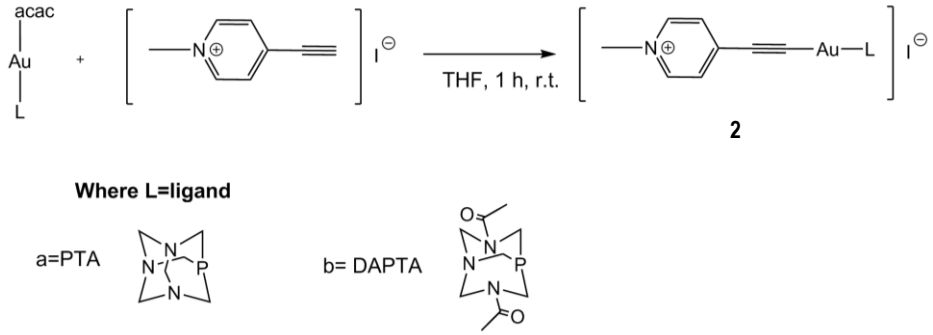

Scheme 3. Synthesis of [Au(N-methyl-4-ethynylpyridine)(L)]I with L= phosphines PTA and DAPTA

The yield for both final complexes was approximately 50 %. To confirm the right structure of the products they were characterized by IR and ^{1}H-NMR in $CDCl_3$ as solvent. The spectra show the expected signals for these complexes, which demonstrate their correct synthesis.

6.1.2. SYNTHESIS OF [AU(N-METHYL-4-ETHYNYLPYRIDINE)(L)](OSO$_2$CF$_3$)

The synthesis of these complexes was performed using the same synthetic route that for iodide ones[36]. N-methyl-4-ethynylpyridinum triflate is obtained by methylation of 4-ethynylpyridine, but using methyl triflate as the methylating agent (Scheme 4) instead of methyl iodide. It was not necessary to synthetize it, as it was provided by the research group.

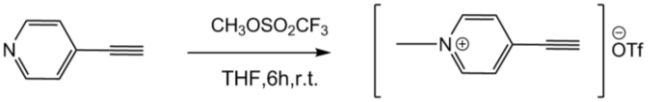

Scheme 4. Synthesis of N-methyl-4-ethynylpyridine triflate

The subsequent coordination to the gold (I) precursor was done in the same way than for **2a** and **2b** complexes:

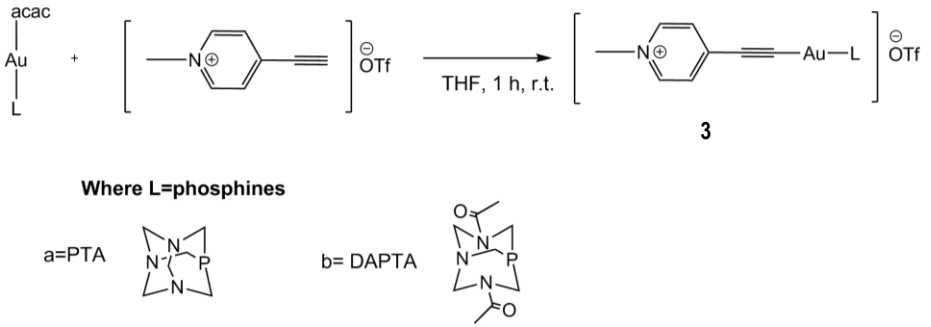

Scheme 5. Synthesis of [Au(N-methyl-4-ethynylpyridine)(L)]OTf

The yield of the last reaction was over 70% for both phosphines so, in general terms, the overall yield of the triflate compound is much higher than for the iodide one. The final products were characterized by IR and ^{1}H-NMR. The spectra show the expected signals for these complexes, which demonstrate their correct synthesis.

6.1.3. SYNTHESIS OF [AU(N-METHYL-4-ETHYNYLPYRIDINE)(L)](CLO$_4$)

The first step to synthetize **4a-b** would be the obtaining of N-methyl-4-ethynylpyridine perchlorate, and its following reaction with [Au(acac)(L)]. In the previous synthesis of compounds **2** and **3**, 4-ethynylpiridine was methylated with methylating agents that introduced directly the desired counterion (See schemes 1 and 4) to obtain N-methyl-4-ethynylpyridine iodide/triflate. Given that no methylating agents that could generate directly the perchlorate counterion are known, the insertion of ClO_4^- should be done by ion exchange (Scheme 6).

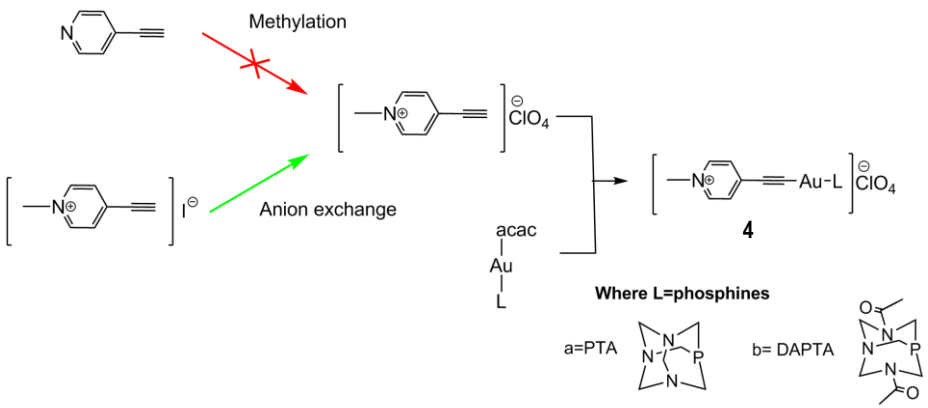

Scheme 6. Schematic synthesis of [Au(N-methyl-4-ethynylpyridine)(L)](ClO_4)

In order to exchange the anion several methods were tried. According to literature[31], the anion exchange could be achieved by treating N-methyl-4-ethynylpyridine iodide with 70% ethanolic perchloric acid, but the detailed procedure was not specified. Therefore, 30 mg of N-methyl-4-ethynylpyridine iodide was dissolved in 1 ml of a mixture 1:9 EtOH/60% perchloric acid. Immediately the solution turned black and an oily precipitate was formed and filtrated. Very small quantity was obtained, though enough to record an IR spectrum (Figure 10). A broad band at 1100 cm^{-1}, which we strongly believe is related to Cl-O stretching of the perchlorate, is observed. Another band at 2108, corresponding C≡C, confirms the presence of the alkynyl moiety. In order to improve the yield of the reaction different solvents were added to the filtrate solution, but it didn't result.

Finally, the solution was evaporated to dryness and a black oily solid was obtained. After cleaning the solid with methanol, though, it turned dark green. An IR spectrum confirmed that the reaction went back and the compound was not the perchlorate salt, but the iodide one.

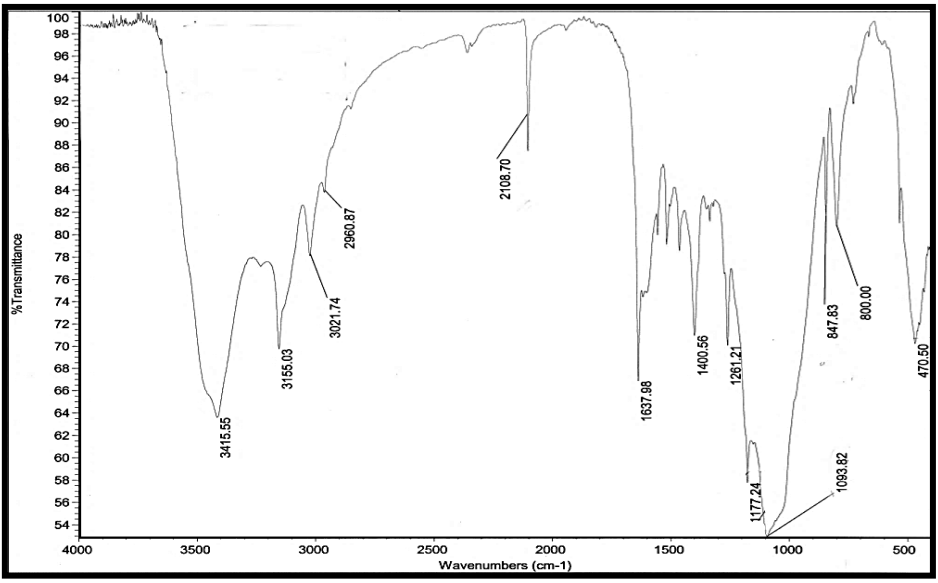

Figure 10. IR spectrum of compound N-methyl-4ethynylpyridine perchlorate

In a second attempt, a different method was used. N-methyl-4-ethynylpyridine iodide was treated with 1 ml of the ethanolic perchlorate solution, and silver perchlorate was added stoichiometrically (Scheme 7). A massive pale brown-coloured precipitate appeared.

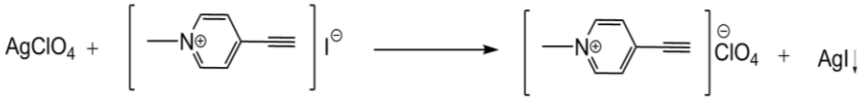

Scheme 7. Synthesis of N-methyl-4-ethynylpyridine perchlorate by anion exchanange.

Given that *Kps*(AgI)=$3 \cdot 10^{-17}$ and *Kps*($AgClO_4$)>1, it was expected that AgI precipitated while N-methyl-4-ethynylpyridine perchlorate was in solution. Nevertheless, after filtering the solution and evaporating the solvent, almost no solid was obtained, so the product couldn't be characterized. Since there was not enough time, no more attempts could be carried out, so it is still pending the synthesis of N-methyl-4-ethynylpyridine perchlorate.

6.2. POLARITY EFFECT ON THE LUMINESCENT PROPERTIES

It has been observed that solutions of complexes **2a-b** and **3a-b** in different solvents present different colours (solvatochromism). Absorption and emission spectra will be performed in order to analyse the variation of the absorbance and emission maxima as a function of the solvent polarity. To that purpose, $5 \cdot 10^{-5}$ M solutions of compounds **2a-b** and **3a-b** in water, acetonitrile, methanol, THF, chloroform, toluene and cyclohexane were prepared and analysed. Absorption spectra were recently recorded in the research group[25] but they were repeated to select the adequate excitation wavelength to analyse the possible polarity effect on the emission. As it can be seen in figure 6, solutions change their colour depending on the solvent and, in some cases, over time. The absorption spectra of compound **3a** in water were recorded in successive days, and it shows a decrease in the band at 390 nm. This variation might be due to the aggregation, and consequent disappearance of the monomeric form, which would be responsible for the absorption, but more studies should be done to confirm this hypothesis. For that reason and to avoid the differences caused by the influence of time all the measurements were recorded with freshly prepared solutions.

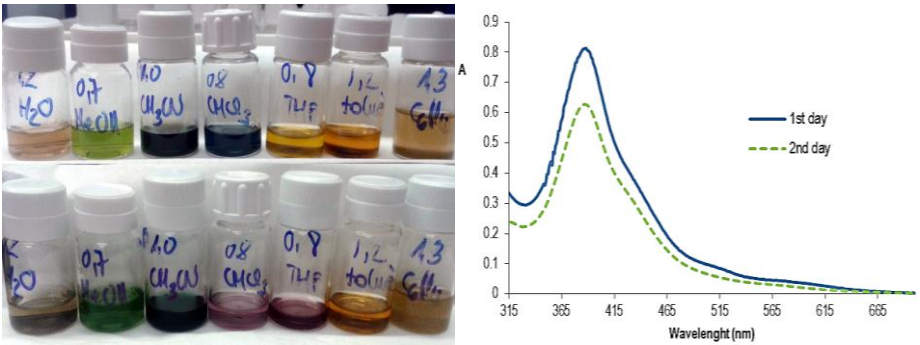

Figure 11. Left, solutions of **3a** in different solvents . At first day (up) and 10 days after their preparation (down). Right, variation in the absorption spectra of compound **3a** in consecutive days due to aggregation

In general terms, the absorption spectra show a complex structure with several bands in the wavelength range from 200 to 700 nm. For **2a** and **3a** derivatives (containing PTA phosphine) there is an important absorption band in the range from 360 to 460 nm, and for **2b** and **3b** (containing DAPTA phosphine) in the range from 290 to 355 nm approximately, depending on the solvent. As polarity increases (view table 1) these bands shift to higher energy (what is called negative solvatochromism, Figure 12), meaning that the excited state of the compound is more stable in non-polar solvents. The sensitivity to solvent polarities of the solvent might indicate the charge transfer character of the transition. In particular, as no differences are observed between complexes with I^- or OTf^-, the transition is thought to be MLCT. These transitions involve promotion of an electron from an orbital that is predominantly metal in character to an orbital that is predominantly ligand.

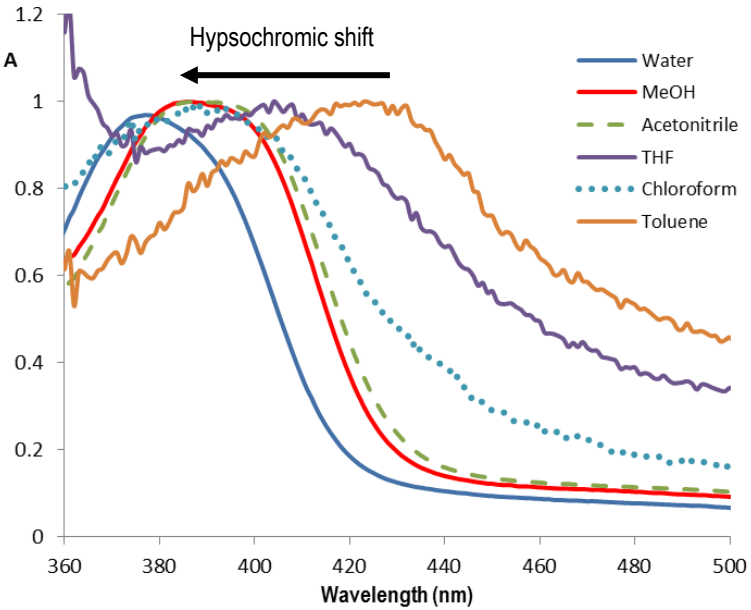

Figure 12. Normalized absorbance spectra of complex **2a** in different solvents in the range of 360-500 nm

Solvent	ε_r
Water	80.1
Acetonitrile	37.5
Methanol	32.7
Tetrahydrofuran	7.6
Chloroform	4.81
Toluene	2.38
Ciclohexane	2.02

Table 1. Polarity of the solvents used according to their dielectric constants

The emission spectra exciting at the longest absorption wavelength (*ca.*380 nm) show two bands at *ca.* 450nm and *ca.* 550nm for all complexes (Figure 13). The general tendency is that as polarity decreases the emission at 600 nm falls and the emission at 450 rises. In the most non-polar solvents as chloroform, THF and cyclohexane the band at 550-600 nm drastically disappears. A hypothesis is that both bands correspond to different types of aggregates. Nevertheless, by comparison with complexes **1a-b** it is likely that band at *ca.* 450 nm is related to the monomer while band at *ca.* 600 nm correspond to the aggregate. Moreover, it could be seen that the emission spectra recorded in cyclohexane (most non-polar solvent) displays a different profile with a vibrionically structured band. This shape could be attributed to the emission of the non-aggregate sample (monomer) in agreement with previous works[17]. This interesting finding could indicate that, in fact, aggregation only happens in polar conditions. The broad emission bands observed in other cases may be attributed to the formation of different types of aggregates, in agreement with the excitation spectra, that show two bands at *ca.* 350 nm and 400 nm respectively (both suggested to be mainly based on σ^*(Au-Au) $\rightarrow \pi^*$ transitions[18]). More analysis is required to find out the effects of the interaction solute-solvent, which are responsible of solvatochromism.

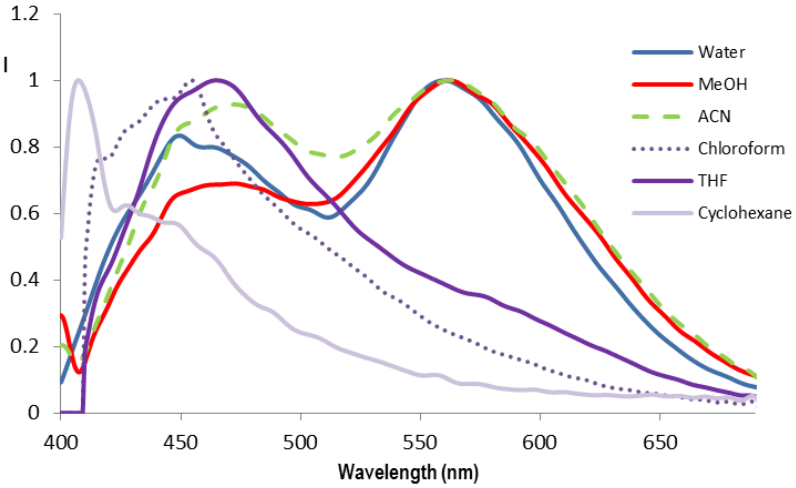

Figure 13. Normalized emission spectra of compound **3a** in different solvents

6.3. OPTICAL MICROSCOPY

The samples were also observed under optic microscopy in order to detect what kinds of aggregates are formed in different solvents. With that purpose some of the samples used in the solvatochrosmim study (with different polarity solvent medium) were dried on appropriate supports prior to the analysis. In particular, samples in water, chloroform and cyclohexane were chosen, though in the last solvent almost nothing was observed, probably due to the low solubility of the complexes (or to the expected lack of supramolecular structures formed, in agreement with emission spectra data).

The supramolecular structures observed this way include dendrimers, short fibres and vesicles with different shapes with lengths up to 10 μm (Figure 14). Even different types of aggregates were observed in the same solvent. In general, small fibres or needles appear in chloroform, while vesicles appear in both water and chloroform. Dendrimers were only observed in complex **3a** in water. A plausible hypothesis is that an initial aggregation step leads to the formation of small vesicles which evolve with time rendering the formation of larger aggregates such as fibres, needles and dendrimers in some cases[28]. Surprisingly, in water the vesicles observed had a spherical shape, while in chloroform they presented the shape of a perfect hexagon. Other geometrical shapes like squares were also observed in some cases. An interesting fact is that around the vesicles there is a short, empty space unoccupied by other smaller aggregates. That might indicate that some kind of repulsion exists between them. In other cases, two vesicles are bounded, but conserving their spherical shape. Given that in some of these structures light seems to pass through the centre, another hypothesis is that these spherical structures are capsules, which is essentially like a vesicle with a hole.

The wide range of aggregate types might be the reason for the little reproducibility of experiments involving these molecules, as each of them might have different, specific properties. More experiments are needed in order to understand if it is possible to predict and understand which are the driving forces responsible of the formation of some supramolecular aggregates instead of the others.

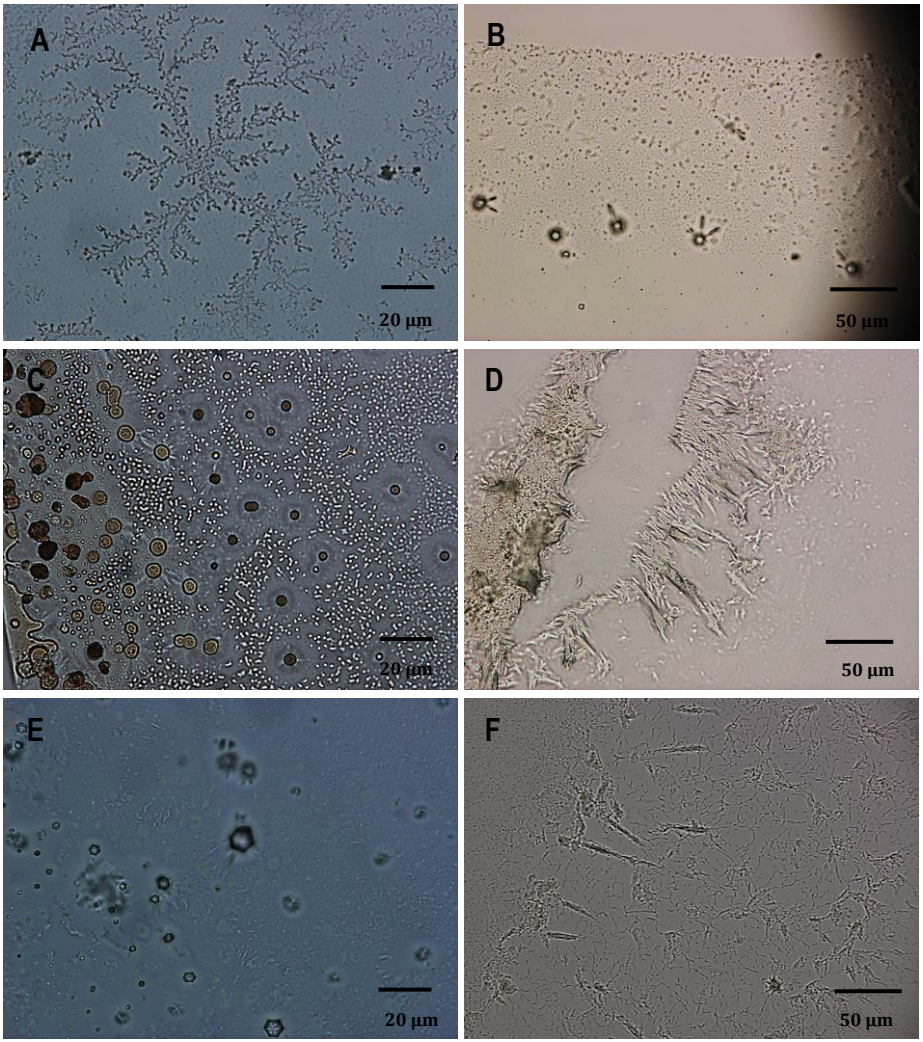

Figure 14. Optical microscopy images of a) **3a** water sample b) **3b** chloroform sample c) **2b** water sample d) **2b** chloroform sample e) **2a** chloroform sample f) **3b** chloroform sample

7. EXPERIMENTAL SECTION

7.1. MATERIALS AND METHODS

General procedures. All manipulations were performed under prepurified N_2 using Schlenk techniques. All solvents were distilled from appropriated drying agents. Deuterated solvents were obtained from Aldrich and were used as received except for $CDCl_3$, which was dried with alumina under nitrogen atmosphere. Solvents used were Milli-Q, methanol p.a. (Fluka), acetonitrile p.a. (Fluka), tetrahydrofuran (Panreac), chloroform p.a. (Fluka), toluene (Merck) and cyclohexane p.a. (Panreac).Commercial reagents, Mg_2SO_4 (Aldrich), CuI (Aldrich), acetylacetonate (Aldrich), 1,3,5-Triaza-7-phosphaadamantane (PTA, Aldrich 97%), 3,7-Diacetyl-1,3,7-triaza-5-phosphabicyclo[3.3.1]nonane (DAPTA, Aldrich 97%), 4-bromopyridine·HCl (Aldrich), Tetrachloroauric acid (Aldrich), Iodomethane (Fluka >99%), $Eu(NO_3)_3{\cdot}5H_2O$ (Aldrich), $Yb(NO_3)_3{\cdot}5H_2O$ (Aldrich), $Dy(NO_3)_3{\cdot}nH_2O$ (Aldrich). Literature methods were used to prepare 4-ethynylpyridine [30] , N-methyl-4-ethynylpyridine iodide [31] , N-methyl-4-ethynylpyridine triflate [36], [AuCl(tht)] [34], [AuCl(PTA)] [32], [AuCl(DAPTA)] [33], [Au(PTA)(C≡$C_5H_4NCH_3$)]I [20] and [Au(DAPTA)(C≡$C_5H_4NCH_3$)]I [20]. Compounds [Au(acac)(DAPTA)] and N-methyl-4-ethynylpyridine triflate were provided by the research group.

Physical Measurements. Infrared spectra were recorded on an IR-Avatar 330 FT-IR Thermo Nicolet. ^{1}H-RMN and ^{31}P{^{1}H}-RMN spectra were obtained on a Varian Mercury 400 and Bruker 400. ElectroSpray-Mass Spectra (+) were recorded on a Fision VG Quatro spectophotometer. UV-Visible Varian Cary 100 Bio spectophotometer was used to acquire absorption spectra. NanoLog™-Horiba Jobin Yvon spectrofluorimeter was used to record the fluorescence emission spectra. Different length path quartz cells (2mm, 4mm and 10mm) were used. Optical microscopy images were acquired on a Olympus BX51 .

7.2. SYNTHESIS OF GOLD(I) COMPLEXES WITH IODIDE AS THE COUNTERION

7.2.1. Synthesis of 2-methyl-4-(4-pyridyl)-3-butyn-2-ol

2-methyl-3-butyn-2-ol (2.4 ml; 24.6 mmol) was added to a solution of 4-bromopyridine (4 g; 20.6 mmol) in diethylamine (25 ml). Catalytic amounts of $[PdCl_2(PPh_3)_2]$ (0.134 g) and copper iodide (0.0247 g) were added. After 15 minutes of stirring at 0°C, the reaction was left at room temperature overnight. The resulting solution is bright yellow. The solvent is then eliminated under vacuum, and an orange solid was obtained. Water was added and the product was extracted with dichloromethane. The organic layer was dried with $MgSO_4$ and evaporated under vacuum. The solid was purified by silica gel column chromatography using hexane: ethyl acetate (1:4) as the eluent mixture. The first orange coloured fraction is rejected and a second yellow fraction is collected and dried under vacuum to isolate 2.255 g of a pale yellow solid

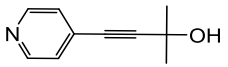

Pale yellow solid. 74% yield. ^{1}H-NMR ($CDCl_3$, 400.1 MHz, 298 K, δ ppm): δ 8.56 (d, J=6.0 Hz, 2H, $H_{\alpha\text{-pyr}}$), 7.27 (d J= 6 Hz, 2H, $H_{\beta\text{-pyr}}$), 2.24 (s, 1H, OH), 1.63 (s, 6H, CH_3).

7.2.2. Synthesis of 4-ethynylpyridine

2-methyl-4-(4-pyridyl)-3-butyn-2-ol (2.255 g, 14 mmol) was dissolved in 27 ml of toluene. NaOH (5 g) was added to the solution and the mixture was refluxed for 2 hours (T= 115 °C). After cooling at room temperature, an insoluble precipitate was removed by filtration. The solvent was then removed under vacuum, and a dark brown solid was obtained. The brown solid was sublimated (T=40 °C) to obtain 0.773 g of a white solid.

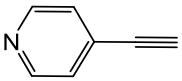

White solid. 53% yield. IR (KBr, cm^{-1}): υ (C≡C) 2100 cm^{-1}. ^{1}H-NMR ($CDCl_3$, 400.1 MHz, 298 K, δ ppm): δ 8.59 (d, J=6.0 Hz, 2H, $H_{\alpha\text{-pyr}}$), 7.34 (d J= 6 Hz, 2H, $H_{\beta\text{-pyr}}$), 3.29 (s, 1H, C≡CH).

7.2.3. Synthesis of N-methyl-4-ethynylpyridine iodide

4-ethynylpyridine (0.200 g, 1.91 mmol) was dissolved in 20 ml of THF and CH_3I (0.25 ml, 4.0 mmol) was added dropwise to the stirring solution. After 48 hours of stirring at room temperature a dark green suspension was obtained. The solid was isolated by filtration and dried under vacuum to obtain 0.250 g of a dark green solid.

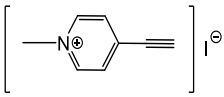

Dark green solid. 53% yield. IR (KBr, cm^{-1}): υ (C≡C) 2104 cm^{-1}. ^{1}H-NMR ($CDCl_3$, 400 MHz): 9.19 (d, J=6.5 Hz, 2H, $H_{\alpha\text{-pyr}}$), 7.98 (D, J=6.0 Hz, 2H, $H_{\beta\text{-pyr}}$), 4.61 (s,3H, N-CH_3), 3.92 (s, 1H, C≡C-H).

7.2.4. Synthesis of [AuCl(tht)]

$HAuCl_4$ (5 g, 16.7 mmol) was dissolved in a water-ethanol solution (6.5 ml / 32 ml). Tht (1.8 ml, 20.4 mmol) was then added dropwise to the previous stirring solution. A yellow solid precipitates immediately. After 30 min of stirring the precipitate is filtrated with a glass disc and dried under vacuum to obtain 0.805 g of a white solid.

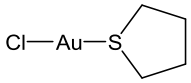

White solid. 75% yield. IR (KBr, cm^{-1}): υ (C-C) 1425 cm^{-1}. ^{1}H-NMR ($CDCl_3$, 250 MHz): δ 3.45 (broad s, 1H, S-CH_2), δ 2.18 (broad s, 1H, S-CH_2-**CH_2**).

7.2.5. Synthesis of [AuCl(PTA)]

1,3,5-Triaza-7-phosphaadamantane (PTA) (0.207 g, 1.31 mmol) was added to a solution of AuCl(tht) (0.420 g, 1.31 mmol) in 40 ml of dichloromethane. After 1 hour of stirring at room temperature the solution was concentrated to half volume and 20 ml of hexane was added to precipitate of a white solid. It was isolated by filtration and dried under vacuum to obtain 0.270 g.

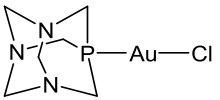

White solid. 53 % yield. ^{1}H NMR ($CDCl_3$, 400 MHz): δ 4.57 (d, J=13.0 Hz, 3H, N-CH_A-N), 4.50 (d,J=13.0 Hz, 3H, N-CH_B-N), 4.28 (s, 6H, N-CH_2-P).

7.2.6. Synthesis of [AuCl(DAPTA)]

3,7-Diaceyl-1,3,7-triaza-5-phosphabicyclo [3.3.1.] nonane (DAPTA) (0.2 g, 0.87 mmol) was added to a solution of [AuCl(tht)] (0.420 g, 1.31 mmol) in 40 ml of dichloromethane. After 1 hour of stirring at room temperature the solution was concentrated to half volume and 20 ml of hexane was added to precipitate a white solid. It was isolated by filtration and dried under vacuum to obtain 0.321 g.

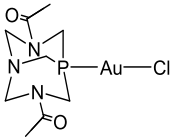

White solid. 81% yield. IR (KBr, cm^{-1}): υ (C=O) 1635 cm^{-1}. ^{1}H-NMR ($CDCl_3$, 400 MHz): δ 5.80 (d, *J* = 14.4 Hz, 1H, N-CH_2-N), 5.70 (dd, *J* = 16.1/8.8 Hz, 1H, N-CH_2-P), 4.96 (d, *J* = 14.2 Hz, 1H, N-CH_2-N), 4.83-4.64 (m, 2H, N-CH_2-P + N-CH_2-N), 4.25 (dt, *J* = 15.5/3.0 Hz, 1H, N-CH_2-P), 4.09 (d, *J* = 14.2 Hz, 1H, N-CH_2-N), 3.97 (s, 2H, N-CH_2-P), 3.67 (dt, *J* = 15.9/4.0 Hz, 1H, N-CH_2-P), 2.12 (s, 6H, CO-CH_3).

7.2.7. Synthesis of [Au(acac) (PTA)]

All the manipulations were done protecting the mixture from the light with aluminum foil in order to avoid decomposition. Solid Tl(acac) (0.114 g, 0.37 mmol) was added to a stirring suspension of [AuCl(PTA)] (0.148, 0.32 mmol) in 15 ml of acetone. After 4 days of stirring at room temperature the solution was filtrated with zelite and concentrated to half volume. 30 ml of n-hexane was added precipitate a white solid, which was filtrated and dried under vacuum. A second and a third fraction of solid was obtained from mother liquor with global amount of 0.053 g of solid.

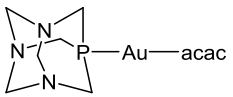

White solid. 31% yield. IR (KBr, cm^{-1}): υ (C=O) 1615 cm^{-1}. ^{1}H NMR ($CDCl_3$, 400 MHz): δ4.52 (AB, q, *J*=13.6 Hz, 6H, N-CH_2-N), 4.19 (s, 6H, N-CH_2-N), 2.46 (d, J_{H-P}=11.6 Hz, 1H, CH_3-(CO)-CH-(CO)-CH_3), 2.30-1.91 (m, 6H, CH_3-(CO)-CH-(CO)-CH_3).

7.2.8. Synthesis of [Au (C≡CC$_5$H$_4$NCH$_3$) (PTA)]I

N-methyl-4-ethynylpyridine iodide (0.013 g, 0.053 mmol) was dissolved in 5 ml of THF. [Au(acac)(PTA)] was added (0.022g, 0.048 mmol) to the stirring solution, which immediately turned wine red colour. After 1 hour of stirring at room temperature the solution was concentrated to half volume and 10 ml of Et_2O were added to precipitate a red solid. It was isolated by filtration and dried under vacuum to obtain 0.030 g of a red solid.

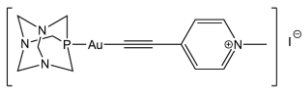

Red solid. 51 % yield. IR (KBr, cm^{-1}): υ (C≡C) 2106, cm^{-1}, υ (C=N) 1637 cm^{-1}. ^{1}H NMR ($CDCl_3$, 400 MHz, δ ppm): δ 4.53 (d, *J*=13.4 Hz, 3H, N-CH$_A$-N), 4.48 (d, *J*=13.6 Hz, 3H, N-CH$_B$-N) , 4.29 (s, 6H, N-CH$_2$-P), 4.19 (s, 3H, N-CH$_a$).

7.2.9. Synthesis of [Au (C≡CC$_5$H$_4$NCH$_3$)(DAPTA)]I

N-methyl-4-ethynylpyridine iodide (0.010 g, 0.040 mmol) was dissolved in 5 ml of THF. [Au(acac)(PTA)] was added (0.021g, 0.045 mmol) to the stirring solution, which immediately turned wine red colour. After 1 hour of stirring at room temperature the solution was concentrated to half volume and 10 ml of Et_2O were added to precipitate a red solid. It was isolated by filtration and dried under vacuum to obtain 0.012 g of a red solid.

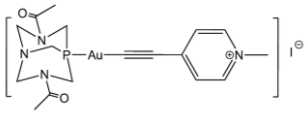

Red solid. 49% yield. IR (KBr, cm^{-1}): υ (C≡C) 2100, cm^{-1}, υ (C=N) 1634 cm^{-1}. ^{1}H NMR ($CDCl_3$, 400 MHz, δ ppm): δ 5.80 (d, *J*=14.3 Hz, 1H, N-CH$_2$-N), 5.69-5.62 (m, 1H, N-CH$_2$-P) , 4.96 (d, *J*=14.0 Hz, 1H, N-CH$_2$-N), 4.70-4.62 (m, *J*=14.3 Hz, 2H, N-CH$_2$-P + N-CH$_2$-N), 4.15 (d, *J*=13.1 Hz, 1H, N-CH$_2$-P), 4.08 (d, *J*=14.3 Hz, 1H, N-CH$_2$-N), 3.88 (s, 2H, N-CH$_2$-P), 3.74 (m, 1H, N-CH$_2$-P), 2.12 (s, 6H, CO-CH$_3$).

7.3. SYNTHESIS OF GOLD(I) COMPLEXES WITH TRIFLATE AS THE COUNTERION

7.3.1. Synthesis of [Au(C≡CC$_5$H$_4$NCH$_3$)(PTA)](OSO$_2$CF$_3$)

N-methyl-4-ethynylpyridine triflate (0.022 g, 0.080 mmol) was dissolved in 5 ml of THF. [Au(acac)(PTA)] was added (0.030g, 0.066 mmol) to the stirring solution, which immediately turned black. After 1 hour of stirring at room temperature the solution was concentrated to half volume and 10 ml of Et$_2$O were added to precipitate a red solid. It was isolated by filtration and dried under vacuum to obtain 0.030 g of a dark green solid.

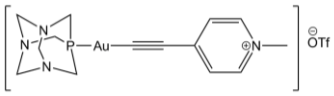

Dark green solid. 71 % yield. IR (KBr, cm^{-1}): υ (C≡C) 2109, cm^{-1}, υ (C=N) 1636 cm^{-1}. ^{1}H NMR (CDCl$_3$, 400 MHz, δ ppm): δ 8.53 (d, *J*=5.9 Hz, 2H, H$_{α\text{-pyr}}$), 7.87 (d, *J*=6.2 Hz, 2H, H$_{β\text{-pyr}}$) , 4.66-4.17 (m, 15H, N-CH$_2$-N+ N-CH$_2$-P+N-CH$_3$).

7.3.2. Synthesis of [Au(DAPTA)(C≡CC$_5$H$_4$NCH$_3$)](OSO$_2$CF$_3$)

N-methyl-4-ethynylpyridine triflate (0.022 g, 0.080 mmol) was dissolved in 5 ml of THF. [Au(PTA)(acac)] was added (0.030g, 0.066 mmol) to the stirring solution, which immediately turned black. After 1 hour of stirring at room temperature the solution was concentrated to half volume and 10 ml of Et$_2$O were added to precipitate a red solid. It was isolated by filtration and dried under vacuum to obtain 0.030 g of a dark green solid.

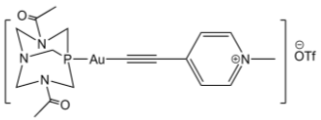

Dark green solid. 78 % yield. IR (KBr, cm^{-1}): υ (C≡C) 2116, cm^{-1}, υ (C=N) 1635 cm^{-1}. ^{1}H NMR (CDCl$_3$, 400 MHz, δ ppm): δ 8.64 (d, *J*=7.1 Hz, 2H, H$_{α\text{-pyr}}$), 7.79 (d, *J*=6.7 Hz, 2H, H$_{β\text{-pyr}}$) , 5.72 (d, *J*=16.0 Hz, 1H, N-CH$_2$-N), 5.60-5.49 (m, 1H, N-CH$_2$-P), 5.08 (d, *J*=13.3 Hz, 1H, N-CH$_2$-N), 4.75 (d, *J*=13.7 Hz, 2H, N-CH$_2$-P+N-CH$_2$-N), 4.31-4.18 (m, 1H, N-CH$_2$-P), 4.03 (s, 2H, N-CH$_2$-P), 3.72-3.51 (m, 1H, N-CH$_2$-P), 2.11 (m, 6H, CO-CH$_3$).

7.4. ABSORPTION AND EMISSION MEASUREMENTS

7.4.1. Solution preparation and materials

*7.4.1.1. Aggregation studies on complexes **1a-b***

$5 \cdot 10^{-4}$ M solutions of compounds **1a** and **1b** were prepared by dissolving 3 mg of each one in 10 ml of water. Solution 10^{-4} M was prepared by diluting 1:5 in water the later solution. $2.5 \cdot 10^{-5}$ and $5 \cdot 10^{-4}$ M solutions were prepared by corresponding dilutions from the previous concentrated solutions. Milli-Q water was used to prepare solutions.

*7.4.1.2. Solvatochromic studies of complexes **1a-b*** in D_2O-DMSO

1mg of compounds **1a** and **1b** were added in 6 different vials each. In all the six vials 0.7 ml of solvents in the following proportions were added: 100% D_2O, 90:10 D_2O/DMSO, 50:50 D_2O/DMSO, 30:70 D_2O/DMSO, 10:90 D_2O/DMSO, 100% DMSO. ^{1}H-NMR , ^{31}P-NMR, absorption and emission spectra were recorded for each sample. The solvents used were D_2O and DMSO-d6.

7.4.1.3. Molecular recognition studies

750 µL of $5 \cdot 10^{-4}$ M solutions of complexes **1a** and **1b** (preparation described in section 7.3.1.1.) were introduced in a 2mm fluorescence quartz cell. Successive additions of 2.5 µL of solutions 0.05M of $Eu(NO_3)_3$, $Yb(NO_3)_3$ or $Dy(NO_3)_3$ were done, and the corresponding absorption and emission spectra were recorded. Solutions 0.05 M were prepared dissolving 0.0214 g of europium nitrate, 0.0224 g of ytterbium nitrate and 0.0174 g of dysprosium nitrate (previously dried) respectively in 5 ml of water. The compounds used were $Eu(NO_3)_3$, $Yb(NO_3)_3$, $Dy(NO_3)_3$ as the analytes and doubled-distilled water as the solvent.

*7.4.1.4. Polarity effect studies of complexes **2a-b, 3a-b***

1 mg of complexes **2a, 2b, 3a** and **3b** was dissolved in 5 ml of methanol. 449 µL of 1a, 461 µL of 1b, 465 µL of 2a and 475 µL of 2b were added in seven different vials each one. The solvent was left to evaporate and then 3ml of each solvent were added in the vials containing the dried solid (final concentration $5 \cdot 10^{-5}$ M). Thus were obtained twenty-eight vials, seven for each complex. Absorption and emission measurements were recorded immediately after their preparation. Solvents used were Milli-Q, methanol p.a., acetonitrile p.a., tetrahydrofuran, chloroform p.a., toluene and cyclohexane p.a.

7.5. OPTICAL MICROSCOPY

7.5.1. Solution preparation and materials

Three drops of the corresponding samples of complexes **2a-b** and **3a-b** (solutions from polarity effect studies) were placed into a microscope slide and evaporated to dryness. Samples of solvents Milli-Q water, chloroform p.a. (Fluka) and cyclohexane p.a. (Panreac) were used. Microscope magnification: x10, x20, x50 and x100.

8. CONCLUSIONS

Different Au(I) complexes with general formula [Au(N-methyl-4-ethynylpyridine)(L)]X (L=PTA,DAPTA and X=I^- and OTf^-) were successfully synthetized with high purity, following the experimental method previously designed in the research group. The yield of the organic precursors has been also successfully improved. Nevertheless, it was not possible to obtain the perchlorate complex as the ligand could not be prepared through anion exchange from the iodide one.

Solvatochromism studies show that there is a blue shift in the absorbance spectra when polarity increases. No shift has been observed in the emission spectra, but only the variation of the relative intensity of the bands corresponding to the aggregate and monomer species. Characterization through optical microscopy shows that a broad range of aggregates are formed in different solvents and even in the same solvent, ranging from less than 1 μm for the smallest aggregates to more than 30 μm for the biggest . A hypothesis is that in an initial aggregation step small vesicles are formed, which evolve over time leading to the formation of larger aggregates such as fibres, needles and dendrimers. No significant differences were observed for complexes with counterion iodide and triflate, so the impact of the counterion might be minor than expected in the resulting aggregates.

For complexes with general formula [Au(4-ethynylbipyridine)(L)] different aggregation velocities were observed for L= PTA and DAPTA derivatives, which suggest a strong participation of the phosphine in the establishment of weak interactions that induce aggregation. The dependence on the polarity of the solvent has been demonstrated, as in water the complexes aggregate so that bipyridine proton signals are so broad that in ^{1}H-NMR could not be detected. Therefore, it is concluded that several parameters such as time and the solvent polarity can be modulated in order to obtain certain desired aggregates or at least have a certain control over the aggregation process. Finally, molecular recognition studies show that the weak interactions established between these molecules can be modulated in the presence of Eu^{3+}, Dy^{3+} and Yb^{3+}, that is translated in a change in their luminescent properties and, possibly, the formation of new heterometallic complexes.

In spite of the progress done in this research, more studies are required in order to confirm and extend the conclusions mentioned above.

9. REFERENCES AND NOTES

1. Osada, Y.; Kajiwara, K.; Fushimi,T.; Hirasa,O; Hirokawa,Y.; Matsunaga,T.; Shimomura, T.; Wang, L.; Ishida, H. Gels hand book, AcademicPress, San Diego, 2001, Vol. 1–3.
2. Sangeetha, N.M.; Maitra, U. Supramolecular gels: Functions and uses. Chem.Soc.Rev. 2005, 34, 821-836.
3. Pipenbrock, M.O.M.; Lloyd, G.O.; Clarke, N.; Steed, J.W. Metal- and anion-binding supramolecular gels. Chem.Rev. 2010, 110, 1960-2004
4. Peng, K.;Tomatsu,I.; Kros, A. Light controlled protein release from a supramolecular hydrogel. Chem.Commun. 2010, 46, 4094-4096.
5. Saha, S.; Bachl, J.; Kundu, T.; Díaz Díaz, D.; Banerjee, R. Dissolvable metallohydrogels for controlled release: Evidence of a kinetic supramolecular gel phase intermediate. Chem.Commun. 2014, 50, 7032-7035.
6. Tam, A.Y.-Y.; V.W.-W. Recent Advances in metallogels. Chem. Soc. Rev. 2013, 42, 1540-1567.
7. Banerjee, S.; Das, R.K.; Maitra, U. Supramolecular gels “in action”. J.Mater. Chem. 2009, 19, 6649-6687.
8. Segarra-Maset, M.D.; Nebot, V.J.; Miravet, J.F.; Escuder, B. Control of molecular gelation by chemical stimuli. Chem.Soc.Rev. 2013, 42, 7086-7098.
9. Wei, Q.; James, S.L. A metal organic gel used as a template for a porous organic polymer. Chem. Commun. 2005, 12, 1555-1556.
10. Ono, Y.; Nakashima, K.; Sano, M; Kanekiyo, Y.; Inoue, K.; Hojo, J.;Shinkai, S. Organic gels are useful as a template for the preparation of hollow fiber silica. Chem. Commun. 1998, 1477-1478.
11. Li, W.; Kim, Y.; Li, J.; Lee, M. Dynamic self-assembly of coordination polymers in aqueous solution. Soft Matter. 2014, 10, 5231-5242.
12. Ajayaghosh, A.; Praveen, V.K.; Vijayakumar, C.; George, S.J. Molecular wire encapsulated into π organogels: efficient supramolecular light-harvesting antennae with color-tunable emission. Angew. Chem. Int. Ed. 2007, 46, 6260-6265.
13. Dzolic, Z.; Cametti, M.; Dalla Cort, A.; Mandolini, L.; Zinic,M. Fluoride-responsive organogelator based on oxalamide-derived anthraquinone. Chem. Commun. 2007, 3535-3537.
14. Lima, J.C.; Rodríguez, L. Supramolecular Gold Metallogelators: The Key Role of Metallophilic Interactions. Inorganics, 2015, 3, 1-18.
15. Mauro, M.; Aliprandi, A.; Septiadi, D.; Kehra, N.S.; de Cola, L. When self-assembly meets biology: Luminescent platinum complexes for imaging applications. Chem. Soc. Rev. 2014, 43, 4144-4166.
16. Díaz, D.D.; Kühbeck, D.; Koopmans, R.J. Stimuli-responsive gels as reaction vessels and reusable catalysts. Chem. Soc. Rev. 2011, 40, 427-448.
17. Gavara, R.; Llorca, J.; Lima, J. C.; Rodríguez, L. Chem.Commun., 2013, 49, 72.
18. Aguiló, E.; Gavara, R. ; Lima, J.C. ; Rodríguez, L. From Au(I) organometallic hydrogels to well-defined Au(0) nanoparticles. J. Mater. Chem. C, 2013, 1, 5538.
19. Gavara, R.; Aguiló, E; Fonseca Guerra, C.; Rodríguez, L.; Lima, J.C. Inorg. Chem, 2015.
20. Aguiló, E.; Supramolecular structures based on Au(I) luminescent hydrogels, 2013. (Departament de Química Inorgànica, Universitat de Barcelona, Barcelona, Spain).
21. Kaur, R.; Mehta, S.K. Self-aggregating metal surfactant complexes: Precursors for nanostructures, Coordination Chemistry Reviews, 2013.
22. Hebbink, G. Luminescent Materials based on Lanthanide Ions, Enshade, the Netherlands, 2002.
23. Brea Faílde, I. Estructuras supramoleculares de Au (I) con ligandos bipiridina, 2015.
24. Guitart Gil, M. Synthesis and aggregation studies in water of new alkynyl gold (I) compounds, 2015.
25. Buckingham, A.D.; Legon, A.C. ; Roberts, S.M. Principles of molecular recognition, 1993.

26. Baron, R.; McCammon, J. A. "Molecular Recognition and Ligand Binding". Annual Review in Physical Chemistry, 2013, 64: 151–175.
27. Chemwiki.ucdavis.edu/Physical.edu/ Physical_Chemistry/ Spectroscopy/ Electronic_Spectroscopy/ Selection Rules for Electronic Spectra of Transition Metal Complexes/Metal to Ligand and Ligand to Metal Charge Transfer Bands.
28. Shiotsuka, M.; Nishiko, N.; Keyaki, K.; Nozaki, K. Construction of a photoactive supramolecular System based on a platinum (II) bis-acetylide Building block incorporated into a ruthenium (II) polypyridyl complex. Dalton Trans., 2010, 39,1831-1835
29. Yau-Hin Hong, E.; Wong, H.; Wing-Wah Yam, V. Tunable self-assembly properties of amphiphilic phosphole alkynylgold(I) complexes through variation of the extent of the aromatic p-surfaceat the alkynyl moieties, Chem. Commun., 2014, 50, 13272.
30. Dellaciana, L.; Haim, A. J.Heterocycl. Chem., 1984, 21, 607-608.
31. Kalgutkar, S.; Castagnoli, N. J. Med. Chem., 1992, 35, 4165-4174.
32. Phillips, A.; Gonsalvi, L.; Romerosa, A.; Vizza, F.; Peruzzini, M. Coord. Chem. Rev., 2004, 248, 955-993.
33. Vergara, E. et al. Eur.J.Inorg.Chem 2007, 2926-2933.
34. Usón, R.; Laguna, R. Organometallic Sythesis, 1986, 3, 322-342.
35. Vicente, J.; Chicote, M.T. The 'acac method' for the synthesis of coordination and organometallic compounds: synthesis of gold complexes, Coord. Chem. Rev. ,1999, 193–195, 1143–1161.
36. Rubinsztajn, S.; Fife, W.K.; Zeldin, M. Tetrahedron Letters, 1992, 33, n 14, 1821-1824.

9. ACRONYMS

PTA: 1,3,5,Triaza-7-Phosphaadamante)

DAPTA: (3,7- Diacetyl-1,3,7-traiza-5-phosphabicyclo [3.3.1.] nonane)

OTf: triflate, trifluoromethanesulfonate

Tht: tetrahydrothiophene

Acac:acetylacetonate

ACN:acetonitrile

THF:tetrahydrofuran

APPENDICES

APPENDIX 1: ^{31}P-NMR

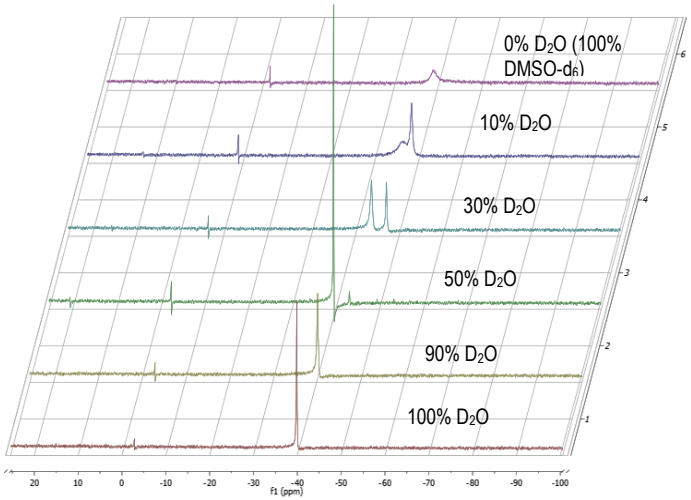

Figure 15. ^{31}P-NMR of complex **1a** in different percentages of D_2O/DMSO-d_6

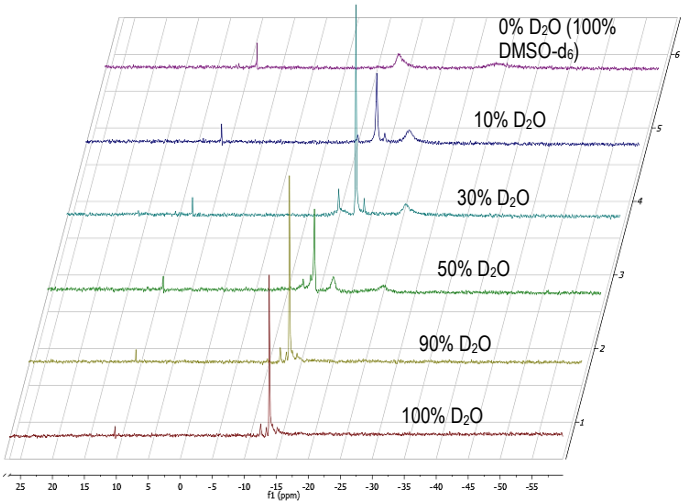

Figure 16. ^{31}P-NMR of complex **1b** in different percentages of D_2O/DMSO-d_6